Geophysical Research Letters

RESEARCH LETTER
10.1029/2024GL110652

Air and Surface Temperatures Differently Drive Terrestrial Carbon and Water Cycles in the High Latitudes

Jing Tang[1,2], Shouzhi Chen[3], David Martín Belda[4], Riikka Rinnan[1], Christian Körner[5], and Yongshuo H. Fu[3,6]

[1]Center for Volatile Interactions (VOLT), Department of Biology, University of Copenhagen, Copenhagen, Denmark, [2]Department of Physical Geography and Ecosystem Science, Lund University, Lund, Sweden, [3]College of Water Sciences, Beijing Normal University, Beijing, China, [4]Karlsruhe Institute of Technology (KIT), Institute of Meteorology and Climate Research, Atmospheric Environmental Research (IMK-IFU), Garmisch-Partenkirchen, Germany, [5]Department of Environmental Sciences, Botany, University of Basel, Basel, Switzerland, [6]Plants and Ecosystems, Department of Biology, University of Antwerp, Antwerp, Belgium

Abstract High-latitude vegetation experience different temperatures than the ambient air temperature. While lacking a regional plant temperature product, we drove the dynamic ecosystem model, LPJ-GUESS, with widely used ERA5-land surface temperature (T_{surf}, at radiative equilibrium) and air temperature to understand ecosystem process responses to these two temperatures. We show that tundra plants' growth is stimulated by warmer T_{surf} in the summer, but in the boreal forests, colder T_{surf} in the non-summer months constrains leaf development and enzyme activity the following growing season. T_{surf} drives higher productivity of tundra plant individuals but leads to less productive individuals in the boreal forest, although with compensatory changes (almost 68%) in vegetation structure. We demonstrate the importance of forcing temperature in simulating high-latitude ecosystem processes and call for a community effort to measure plant temperatures across canopy heights and seasons to reduce uncertainties in estimating high-latitude plant responses and feedback to climate.

Plain Language Summary The temperature experienced by plants often differs from the surrounding air temperature. This plant temperature plays a large role in how plants grow and function. By using two common observation-based temperature data sets (air and surface temperatures) to drive an ecosystem model, we found that warmer summer surface temperatures stimulate tundra plant growth, but colder temperatures in other seasons than summer can limit growth in the boreal forest. We highlight how important it is to use actual temperatures plants in high-latitude ecosystems experience to improve our understanding of how these plants interact with their environment under the changing climate.

Key Points:

- Plant growths in tundra are stimulated by surface temperature which is higher than air temperature in summer months
- Forcing temperature is crucial in determining high-latitude vegetation structure and productivity
- Nor surface or air temperature can sufficiently capture plant temperature dynamics

Supporting Information:

Supporting Information may be found in the online version of this article.

Correspondence to:

Y. H. Fu and J. Tang,
yfu@bnu.edu.cn;
jing.tang@bio.ku.dk

Citation:

Tang, J., Chen, S., Martín Belda, D., Rinnan, R., Körner, C., & Fu, Y. H. (2024). Air and surface temperatures differently drive terrestrial carbon and water cycles in the high latitudes. *Geophysical Research Letters*, *51*, e2024GL110652. https://doi.org/10.1029/2024GL110652

Received 12 JUN 2024
Accepted 29 AUG 2024

Author Contributions:

Conceptualization: Jing Tang, Yongshuo H. Fu
Formal analysis: Jing Tang, Shouzhi Chen, David Martín Belda
Funding acquisition: Jing Tang, Riikka Rinnan, Yongshuo H. Fu
Methodology: Jing Tang, Shouzhi Chen, Yongshuo H. Fu
Supervision: Jing Tang, Riikka Rinnan, Yongshuo H. Fu
Visualization: Shouzhi Chen
Writing – original draft: Jing Tang, Shouzhi Chen

1. Introduction

Air temperature (T_{air}), routinely measured at the height of a few meters above canopies (usually at 2 m) at meteorological stations or simulated by climate models, describes macroclimate conditions for an ecosystem (Aalto et al., 2022; Körner & Hiltbrunner, 2018). T_{air} has been widely used in models (Huang et al., 2019; Smith et al., 2014) to drive ecosystem functions, vegetation biogeography, plant physiology, and disturbances like wildfire. However, T_{air} is usually not the temperature experienced by organisms, such as plants, and we should be aware of bias resulting from using T_{air} to drive some of the ecosystem processes (Jones, 1985; Körner & Hiltbrunner, 2018). The bias magnitude in interpreting thermal responses using T_{air} is strongly linked to process response time; such bias could be larger for thermal responses to heatwaves than for vegetation biogeography distribution (Piao et al., 2019).

The magnitude and temporal variations of T_{air} are clearly distinct from surface temperature (T_{surf}). T_{surf} is defined as the temperature of the solid surface of a landscape and is strongly influenced by surface properties and microclimatic conditions (such as light and moisture levels). Land surface temperature (LST) instantaneously detected by remote sensors is commonly used by the remote sensing community due to its wide coverage (E. J. Good et al., 2017), and the term T_{surf} used here is derived from solving surface energy balance and simulating plant and physical processes (Muñoz-Sabater et al., 2021). T_{surf} can represent the plant-experienced temperature ($T_{plant,}$ can also be called as skin temperature) at the canopy surface for vegetated areas in snow-free months. For non-vegetated areas, T_{surf} describes the temperature at soil/snow surfaces. The differences between these daily maximums of T_{surf} and T_{air} can exceed 20°C (E. J. Good, 2016).

Writing – review & editing: Jing Tang, Shouzhi Chen, David Martín Belda, Riikka Rinnan, Christian Körner, Yongshuo H. Fu

In temperature-limited regions (e.g., tundra, boreal and Alpine ecosystems), it is paramount to apply the correct temperature to understand plant processes and their responses and feedbacks under a fast-changing climate (Körner & Hiltbrunner, 2018; Rinnan et al., 2020; Simin et al., 2021). In-situ field observations from the Arctic and Alpine ecosystems have identified that T_{plant} can be more than 10°C higher than T_{air} measured at 2 m height (Körner, 2007), and the temperature difference is smaller on cloudy days than on sunny days (Scherrer & Köerner, 2010; Simin et al., 2021). The observed differences between these two temperatures can be larger than the projected changes in T_{air} for these cold ecosystems by the end of this century (Still et al., 2019). This greatly challenges the current estimations of the greenhouse gas fluxes and vegetation responses to climate change in the cold regions. The dynamics of T_{plant} are influenced by ambient T_{air} but they are closely interlinked with leaf physiological and morphological properties, canopy structure, radiation intensity, and near-surface aerodynamics (Scherrer & Köerner, 2010). Currently, there are no observation-based regional/global data sets which describe the dynamics and magnitudes of T_{plant}, which hinders a direct evaluation of T_{plant} simulated by land modeling communities.

Gap-free global reanalysis data, which integrate observations from the past and numerical weather forecasting models based on data assimilation, provide a complete and accurate estimation of many global variables about the earth system. The fifth generation European Center for Medium-Range Weather Forecasts Reanalysis (ERA5) generates global 2 m T_{air} and T_{surf} at 0.25° and at hourly scales (Muñoz Sabater, 2019). The 2 m T_{air} describes the near-surface air temperature, while T_{surf} is the temperature of the Earth's surface necessary to achieve radiative equilibrium derived from the surface energy balance (ECMWF, 2016). These two temperatures are widely used to monitor climate change, understand Earth's surface conditions and calibrate/evaluate model outputs and satellite products (La Sorte et al., 2021; Muñoz-Sabater et al., 2021). T_{air} quantifies macroclimate conditions and is primarily influenced by atmospheric processes such as solar radiation, movements of air masses, cloud cover, and atmospheric pressure. T_{surf} is influenced by solar radiation absorption, surface properties and heat dissipation. For vegetated areas, T_{surf} is also influenced by leaf traits, such as color, hairiness and transpiration rate, canopy structure and boundary layer aerodynamics (ECMWF, 2016). Notably, none of these two temperatures can fully represent the average T_{plant} of the whole canopy. Still, we argue that T_{surf}, considering energy exchanges at the canopy level and vertical temperature gradients of air, should be closely linked to plant processes in ecosystems with low-statured vegetation, especially in snow-free seasons. The decoupling of T_{air} and T_{surf} for arctic tundra vegetation is expected due to the low air mixing close to the canopy and/or cold climate-adapted plant traits (Körner, 2021; Scherrer & Köerner, 2010). Capturing this decoupling is essential to understanding the growth conditions of these plants facing rapid climate change (Still et al., 2019).

Here, we aim to quantitatively assess how two widely used temperature products (i.e., ERA5 T_{air} and T_{surf}) influence ecosystem processes at high latitudes by thoroughly examining LPJ-GUESS simulated changes in vegetation production, carbon and water cycling, and vegetation composition. The quantified results are beneficial for raising awareness of model uncertainties related to temperature inputs and contribute to narrowing down model uncertainties in estimating land-atmosphere carbon and water exchanges.

2. Materials and Methods

2.1. LPJ-GUESS Model

LPJ-GUESS is a process-based dynamic global vegetation model (DGVM) that can simulate the carbon, water, and mass cycles and responses to climate and environmental changes (Sitch et al., 2003; Smith et al., 2014). LPJ-GUESS simulates vegetation dynamics based on plant individuals' establishment, mortality, competition, and disturbances at the community level (Hickler et al., 2004; Pugh et al., 2019). The model simulates plant physiological and biogeochemical processes at a daily time step and describes the growth, mortality, disturbances and allometry at an annual time step.

The model simulates at gridcell level, and within each gridcell, different stands are used to represent different landcover types, such as crops, wetlands, pasture, managed forest, and natural vegetation. This study includes natural and wetland landcover classes. Within each stand, the model simulates a number of independent patches (50 in this study), representing different disturbance and succession histories. Within each patch, different individuals compete for the available resources, including light, water and nutrients. The model enables the explicit representation of the canopy vertical structure, mixed plant composition and competition. The simulations over tundra and boreal regions in this study included 23 plant functional types (PFTs, a set of species with similar

responses to the environment and with similar effects on ecosystem functioning): five grass, three bryophytes, eight shrub and seven tree PFTs, see detailed description in Tang et al. (2023) and Rinnan et al. (2020).

In this study, LPJ-GUESS was separately driven by ERA5-land air and surface temperatures (Details in Supporting Information S1 Text S1–S3). As this model version (without surface energy balance) only needs forcing temperature as input, we disentangled the impacts from two ERA5-land temperatures on different processes. The study area, Arctic and boreal regions, mainly consist of boreal needle-leaved evergreen and deciduous trees, upland shrubs, wetland grass and moss. In southern boreal regions, there are also some broad-leaved deciduous trees (see the dominant PFTs in Figure S2 of Supporting Information S1).

2.2. Untangling Contributions From Individual-Level Changes and Community Structural Changes

LPJ-GUESS normally outputs the averaged fluxes or state variables at the gridcell level. In response to different temperatures (i.e., surface and air temperature), the gridcell-outputs, for instance, carbon and water fluxes, could include temperature responses not only from individuals, but also changes in the vegetation community. This could for example, be changes in the numbers of PFT individuals, age and canopy structures. It is thus important to isolate the effects of these two parts to separate the response magnitudes of averaged plant individuals and the changes in vegetation community.

In LPJ-GUESS, individual-level simulations are first carried out to estimate fluxes (e.g., GPP) and update state variables (e.g., leaf area index, LAI), and these fluxes and state variables are then summed or averaged within each patch, considering PFT individual density and canopy structure. To separate these two parts, we assume that the changes in variable values ("X" in the following equation) can be split into the averaged changes at the individual level and the vegetation community structural changes in PFTs within the patch:

$$X_{\overline{indiv}}^{PFT} = \frac{\sum_{indiv=1}^{indiv=n} X_{indiv}^{PFT}}{n} \tag{1}$$

$$K_S^{PFT} = \frac{X_{patch}^{PFT}}{X_{\overline{indiv}}^{PFT}} \tag{2}$$

where the $X_{\overline{indiv}}^{PFT}$ represents the X value (such as GPP) of a given PFT averaged across different individuals in a patch, that is, the averaged state of individual plants, and n is the number of individuals within that patch. K_S^{PFT} is the composition coefficient of a given PFT, X_{patch}^{PFT} representing the patch-level X of a given PFT summed across all individuals, which is the overall state of all individuals of the given PFT in that patch. X_{patch}^{PFT} is the community scale state under the joint action of individual's state and the vegetation community structure.

We then calculated the relative percentage changes of each selected variable (Equations 3 and 4) at the individual and structural levels from these simulations driven by T_{air} and T_{surf}:

$$\Delta X_{\overline{indiv}}^{PFT}(\%) = \frac{X'^{PFT}_{\overline{indiv}} - X_{\overline{indiv}}^{PFT}}{X_{\overline{indiv}}^{PFT}} \times 100\% \tag{3}$$

$$\Delta K_S^{PFT}(\%) = \left[\left(K_S^{PFT'} - K_S^{PFT}\right)/K_S^{PFT}\right] \times 100\% \tag{4}$$

where $\Delta X_{\overline{indiv}}^{PFT}(\%)$ and $\Delta K_S^{PFT}(\%)$ represent the percent changes of individual level GPP and structural composition coefficient for each PFT through comparing simulations driven by T_{surf} and T_{air}. Primed and unprimed quantities refer to the outputs driven by T_{surf} and T_{air}, respectively.

Since the proportion of different PFTs in a gridcell is different, it is necessary to weight the changes of individual level change in X and composition coefficient according to the foliar projection cover (FPC) at the gridcell level:

$$\Delta X_{\overline{indiv}}^{grid}(\%) = \sum_{i=1}^{n} \Delta X_{\overline{indiv},i}^{PFT}(\%) \times FPC_i \tag{5}$$

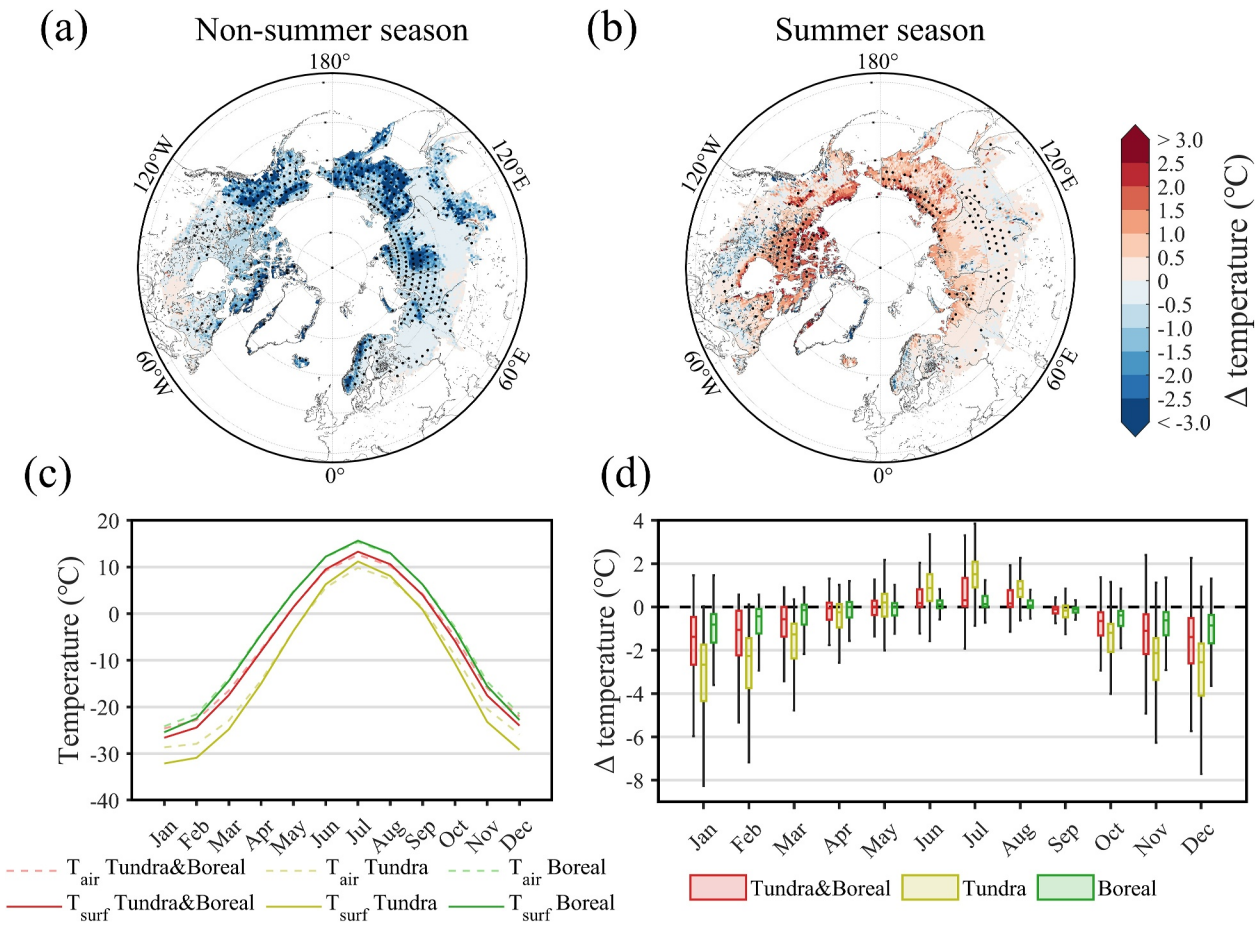

Figure 1. The spatial distribution of the differences between surface and air temperatures for the non-summer season (a, period of the year except June, July and August) and summer season (b, June, July and August) between 1979 and 2015. The monthly means of surface and air temperature (c) and the monthly differences between surface and air temperatures in three regions (d). The boxplots with whiskers show the fifth, 25th, 50th, 75th, and 95th percentiles of the differences between these two temperatures. Tundra & Boreal: including both tundra and boreal biomes. Dots represent the region with significant differences.

$$\Delta K_S^{grid}(\%) = \sum_{i=1}^{n} \Delta K_{S,i}^{PFT}(\%) \times FPC_i \quad (6)$$

Where $\Delta X_{indiv}^{grid}(\%)$ and $\Delta K_S^{grid}(\%)$ are the gridcell-level percentage changes of individuals' X and structural composition coefficient when comparing two simulations, i represents the ith PFT, and FPC_i represents the FPC of the ith PFT.

3. Results and Discussions

3.1. Differences in Surface and Air Temperatures

For 72% of the study region, ERA5 T_{surf} is higher than T_{air} in the summer season (i.e., June, July and August) but lower in the non-summer season (Figures 1a and 1b). The temperature differences (ΔT) of these two periods are much larger in the tundra region compared to the boreal region, likely due to the high albedo of snow-covered tundra in winter and low canopy height and dark surface in summer. This substantial seasonal variability of near-surface temperature in the tundra region is also found in in-situ temperature measurements across 446 study sites in northern Europe (Aalto et al., 2022). Averaging the whole tundra region (based on the tundra extent from *Ecoregions 2017* © Resolve) between 1979 and 2015, the monthly T_{surf} is up to 1°C warmer for the summer season but down to −3°C colder than the T_{air} for the non-summer season (Figure 1c). There are larger spatial variations in

monthly temperature differences over tundra than in boreal regions (Figure 1d). In the Canadian Arctic Archipelago and northern Russia, the summer season average T_{surf} can be over 3°C higher than the reference T_{air}.

3.2. Impacts on Plant Carbon and Phenology

Between 1979 and 2015, simulated values for gross primary productivity (GPP) over the study region were higher by 0.031 PgC/yr (+0.29%) for summer season (i.e., June–August) but lower by 0.13 PgC/yr (−18%) for non-summer season (i.e., the rest of months than June–August), respectively, when driven by T_{surf} instead of T_{air} (see the monthly differences of GPP in Figure S1 of Supporting Information S1 and the dominant PFTs for each gridcell in Figure S2 of Supporting Information S1). The regional GPP increases are primarily contributed by changes from three deciduous plant functional types (PFTs GRT: Tundra Graminoid and Forb, LSS: Low shrub summergreen, and BNS: Boreal needle-leaved summergreen, Figures 2a and 2b). The increases of GPP from GRT and LSS are mainly distributed in the Arctic region, where higher T_{surf} over the summer season (Figure 1b) predominantly stimulates the growth of these PFTs. The increases in GPP from BNS are mainly centered in the northern part of Siberia's larch forest (Figure 2b). In contrast, T_{surf} leads to a clear decrease of GPP for evergreen PFTs over the boreal region (Figure 2c) compared to T_{air} (reduced by −2.44% and −1.92% for boreal needle-leaved evergreen, BNE and boreal shade-intolerant needle-leaved evergreen BINE, respectively). This decrease is likely linked to the colder T_{surf} in non-summer season months, as the T_{surf}-to-T_{air} differences are relatively small for summer season months in this region (Figures 1a and 1d). At the seasonal scale, the reduced GPP for evergreen PFTs driven by a colder T_{surf} outside the main summer season carries over to the summer season (Figure 2a). These carry-over impacts seem to be associated with the colder T_{surf} in spring and winter months, bringing the inhibition effects from the low temperature on C3 photosynthesis and also causing lower annual leaf area index in general, which influences the summertime GPP (Figure S3 in Supporting Information S1 showing the averaged differences of temperature response in photosynthesis and LAI for one gridcell dominated by PFT BNE). The deciduous broad-leaved tree, IBS, also shows a widespread decrease over the southern part of the boreal region.

The choice of driving temperature also causes large differences in the modeled start and end of the growing season, that is, SOS and EOS (Supporting Information S1 Text S2), for many summergreen PFTs (Figures 2d and 2e showing PFTs with dominance for each gridcell and Figures S4 and S5 in Supporting Information S1 show mapped differences in SOS and EOS for all PFTs). T_{surf} drives both earlier and later SOS (smaller and larger SOS in values, respectively) depending on the PFT compared with T_{air}. For example, IBS and TeBS-dominated gridcell in the boreal region show the largest delays (1.1 and 2.0 days, averaged over the study region) at the start of the growing season, while HSS, GRT and SPDS (summergreen prostrate deciduous shrubs)-dominated gridcell in the Arctic region, show an earlier SOS (2.3, 1.7 and 2.1 days, averaged over the study region) when driven by T_{surf}. For EOS, the delays (i.e., later leaf senescence) occur mainly for GRT and SPDS-dominated gridcell, and the opposite (i.e., an earlier EOS) is seen for boreal summergreen PFTs from the T_{surf} simulation.

Overall, we found a longer growing season (period between SOS and EOS, which were determined by Unified model (Sykes et al., 1996) and leaf longevity threshold, respectively) in the Arctic region if T_{surf} was used as the input, while the phenological development of boreal deciduous PFTs seems to be constrained by the relatively colder T_{surf} over the spring and winter months (Figure 1d), causing lower GPP values for PFT IBS (Figure 2e). In spring, snow melting can alter plant-experienced temperature, available water, and canopy vegetation composition D E Winkler et al., 2018). During this temperature-sensitive period, it is essential to account for snow-plant interactions in determining T_{plant} and associated linkages to spring budburst (Vitasse et al., 2021). In autumn, multiple cues, including growth development in growing seasons, autumn radiation and soil moisture conditions, could impact the leaf senescence (Zohner et al., 2023), which LPJ-GUESS does not yet account for (Seyednasrollah et al., 2020). We further argue that the dependence of leaf senescence on spring and growing-season conditions should be further examined by accounting for differences in air and plant temperatures.

3.3. Impacts on Plant Individuals and Canopy Structure

We further attribute the GPP differences at the gridcell level (Figure 3a) to the temperature-induced changes in GPP values averaged across all individuals within each gridcell (hereafter called *individual GPP* changes) and changes in the total coverages and number of PFT individuals (hereafter called *PFT composition* or *PFT structural* changes, see Methods).

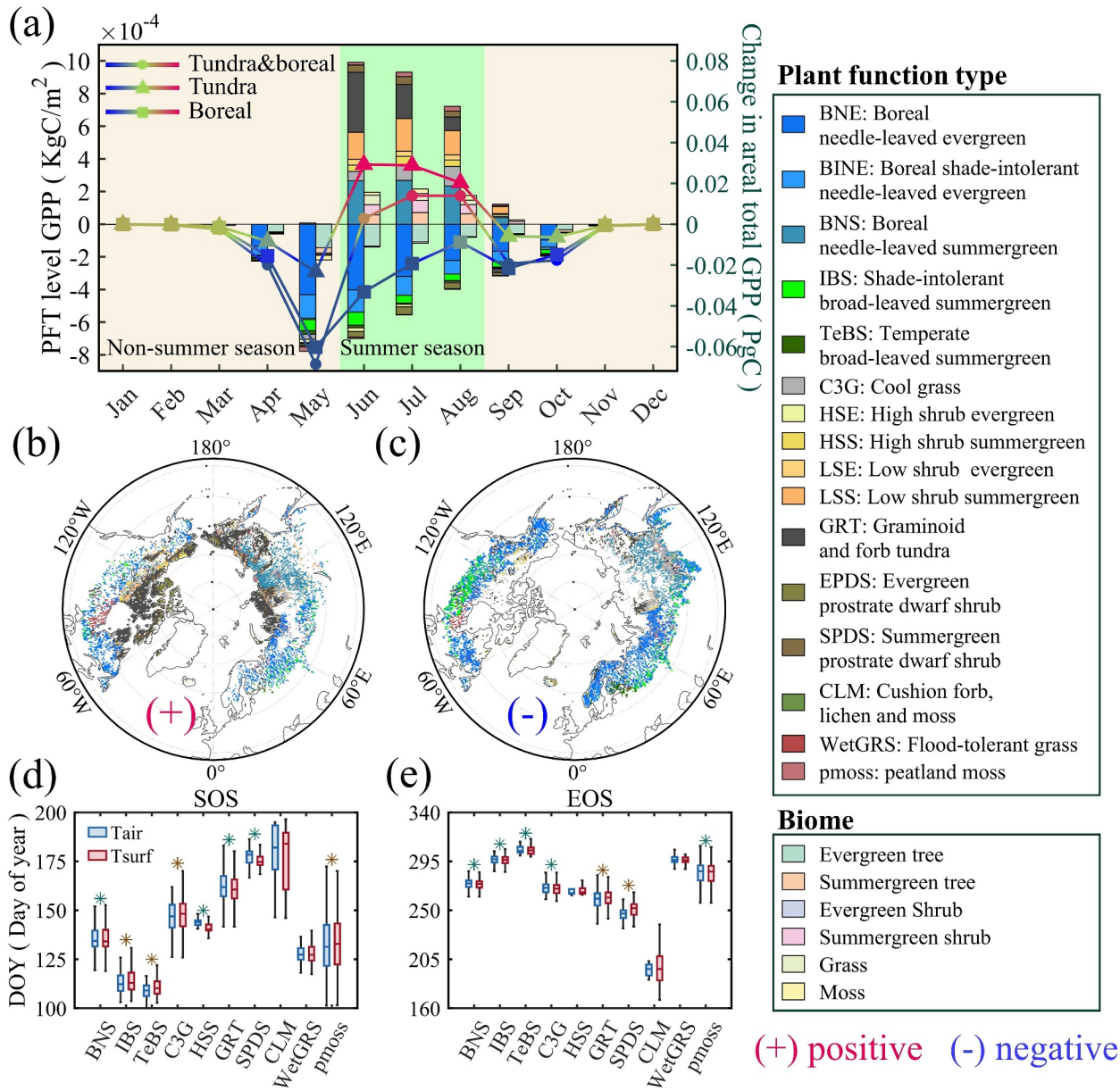

Figure 2. Modeled differences in monthly gross primary production (GPP) and phenology between T_{surf} and T_{air}-driven simulations for different plant functional types (PFTs). (a) Averaged differences in monthly GPP for each PFT or biome (left *y*-axis) and the areal total GPP over the tundra and boreal areas (right *y*-axis). The positive values (in red colors) mean higher areas of total GPP values driven by T_{surf} compared to $T_{air,}$ and vice versa (more in blue colors). The green and light brown backgrounds represent the summer and non-summer season periods, respectively. The spatial distribution of the PFTs that dominate the simulated difference of GPP shown in (a): PFTs' responses for GPP increase (b, +) and decrease (c, −). (d) The simulated start of the growing season (SOS) and (e) end of the growing season (EOS) for deciduous PFTs (only included the gridcells with one of the listed PFTs as the dominant). The asterisk (*) represents significant differences (based on *t*-test) between the two simulations, and green and brown asterisks indicate earlier and later T_{surf}-driven SOS or EOS simulations than that of T_{air}-driven simulations, respectively.

In the Arctic, individuals become more productive (up to 30% increase) when driven by T_{surf} instead of T_{air} (Figure 3b). However, in the boreal region, the model generally predicts lower values of individual GPP, especially over certain areas, for example, Scandinavian mountains and southern Russia, which are largely contributed by the lower GPP of boreal needle-leaved evergreen in these regions (Figure 2e).

PFT structural changes positively or negatively contribute to the GPP changes. The negative contributions of PFT composition changes (reduced number of individuals and/or foliar cover fraction, Figure 3c) to GPP increases occur in the western and middle parts of Russia and parts of Canada. However, the Canadian Arctic Archipelago

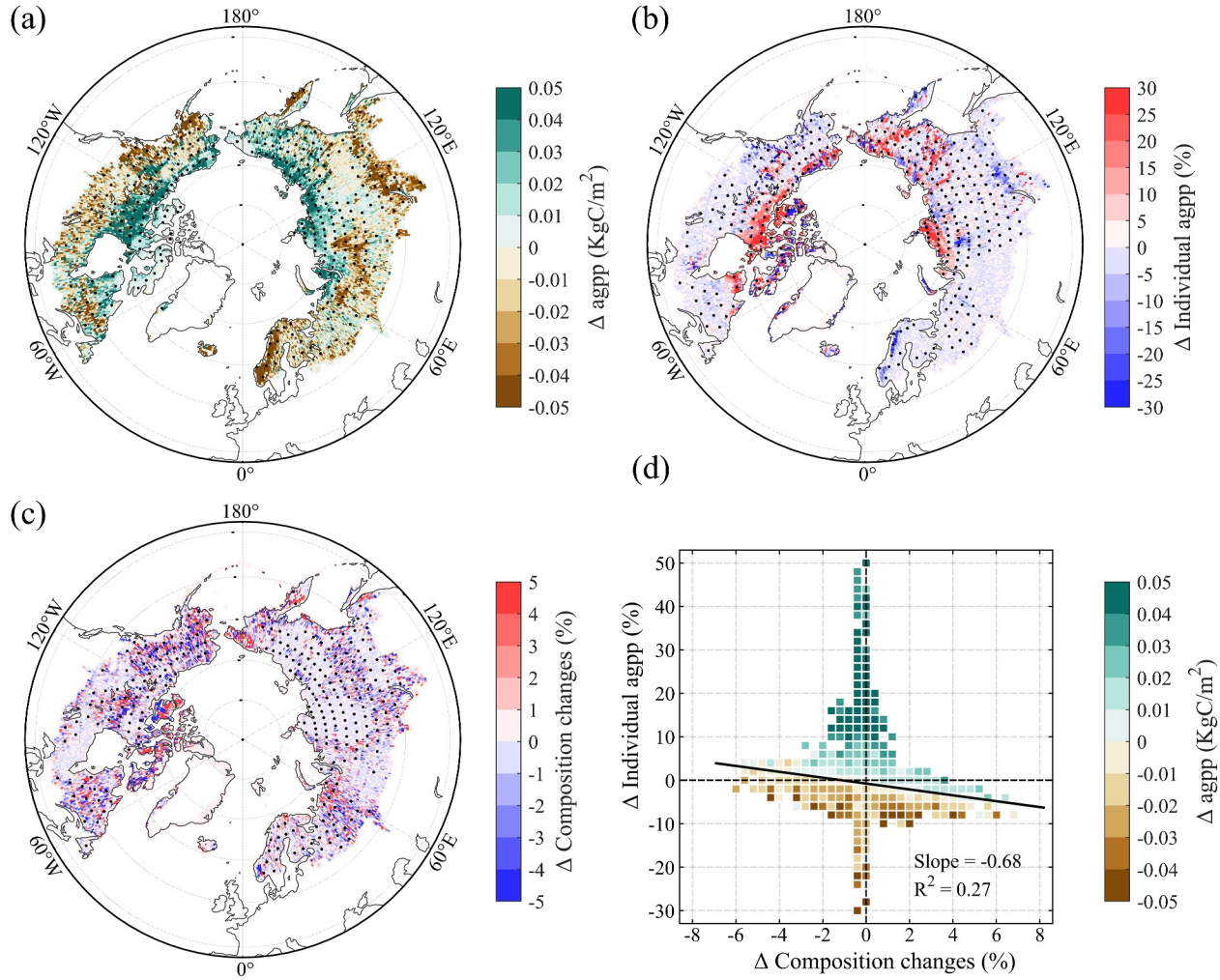

Figure 3. Gross primary productivity (GPP) changes are attributed to individual-level GPP changes and composition changes. (a) The modeled differences in the annual GPP in 1979–2015 at the gridcell level; (b) The averaged changes of GPP at the individual levels; (c) the changes in composition; positive/negative values represent increased or reduced numbers of individuals and/or foliar cover fraction (d) The synergistic impacts of individual GPP changes and composition changes on annual GPP changes, each data point represents the mean value of Δagpp over gridcell within certain interval variation of individual changes of agpp and composition changes. Dots represent the region with significant differences.

experiences a clear positive contribution from PFT composition changes to the GPP increase (Figure 3c). Overall, the contributions from PFT composition changes (Figure 3b) are more patchy than individual GPP changes (Figure 3a).

Over the whole study region, there are clear T_{surf}-induced trade-off impacts on the gridcell-level GPP from individual GPP changes and PFT composition changes. The solid line in Figure 3d shows where the GPP changes induced by the T_{surf}-to-T_{air} differences are zero, and the negative slope (almost 68%) indicates that the changes from individual GPP and the PFT composition tend to cancel out each other. Overall, relatively larger areas (more green dots in Figure 3d) have increased GPP when T_{surf} drives the model compared to T_{air}, and the increase is mainly linked to more productive individuals with lower structural density (green dots on the upper-left quadrant) for the study period 1979–2015. In a longer period, temperature difference-induced vegetation composition changes might increasingly influence ecosystem-level productivity as shifts in vegetation species and densifying canopy take time.

For most of the study region, the simulated changes in actual evapotranspiration (ΔAET) positively correlate to the changes in temperatures (ΔT) for both summer and non-summer seasons (Figures 4a and 4b). Throughout the year, we see apparent increases in monthly AET in the Arctic in summer, in contrast to the spring (April–May)

10.1029/2024GL110652

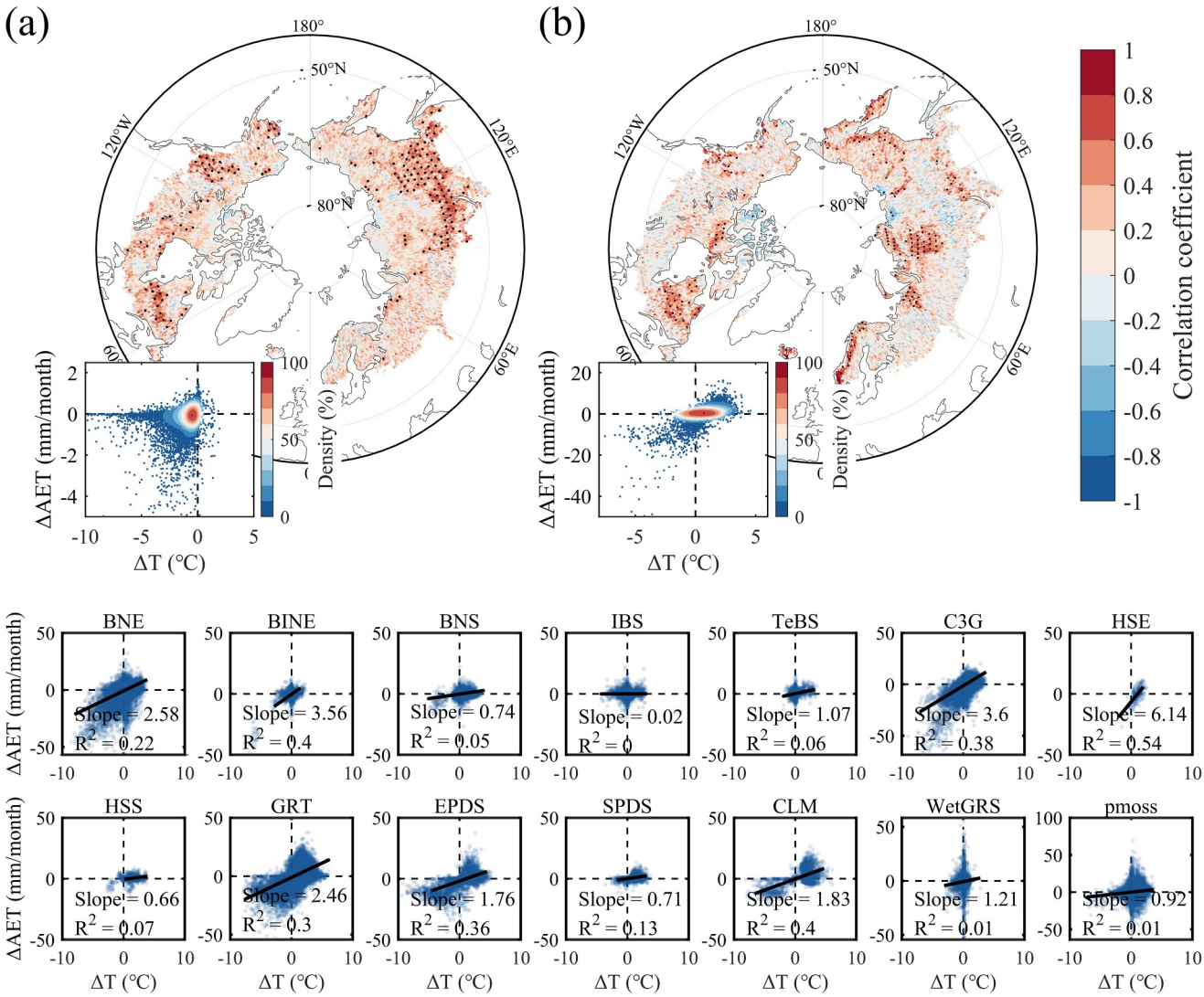

Figure 4. Correlation between changes in actual evapotranspiration (ΔAET) and differences of two temperatures (ΔT) for non-summer (a) and summer seasons (b) between 1979 and 2015. Dots on the map represent regions with significant correlation. (c) Scatter plot of the annual changes in gridcell ΔAET (individual plots based on the dominated PFTs) and ΔT during the summer season.

decreases in monthly AET in boreal region when driven by T_{surf}, not T_{air} (see Figure S6 in Supporting Information S1). There are different sensitivities in PFTs (slopes in Figure 4c) regarding the ΔAET responses to ΔT. The two temperature-induced changes in vegetation composition at each gridcell can contribute to influence the response sensitivities. Generally, the slopes are steeper for evergreen-dominated and grassland areas, indicating stronger ΔT impacts on AET. The strong responses in grassland areas are powered by the large increase in PFT coverage when driven by T_{surf} (Figure S7b in Supporting Information S1).

In LPJ-GUESS, ERA5 T_{air} and T_{surf} resulted in differences in both modeled individual plant status and canopy coverage, and the modeled foliar projective cover (FPC) shows higher vegetation coverage in tundra regions with T_{surf} than T_{air} inputs (Figure S2 and S7 in Supporting Information S1). The increased FPC is mainly a result of an increased coverage of the grass (PFT GRT). FPC mainly decreases in the boreal region, contributed by reduced temperate grass (PFT C3G) and needleleaf trees (PFTs BNE and BNS).

We further analyzed the long-term trends of simulated annual GPP and AET forced by T_{air} and T_{surf}, as well as the trends for simulated differences in GPP and AET between these two runs (Figure S8 in Supporting Information S1). During 1979–2015, both GPP and AET experienced significant increases in large areas of the study domain, and the areas with significant increases are similar between the two runs driven by T_{air} and T_{surf}. For the

trends in simulated GPP differences, 44% of study areas showed significant trends, and among them, the majority (80.5%) showed positive values, meaning increased differences among the two runs. For the trends in simulated AET difference, 31% of study areas showed significant trends, and among them, 72.5% of areas showed enlarged differences among the two runs.

3.4. General Discussions

In thermal-limited tundra and boreal ecosystems, temperature is essential for many plant processes, thermal habitat diversity and ecosystem functions (Scherrer & Köerner, 2010). The often-observed strong decoupling between T_{surf} and reference T_{air} at, for instance, 2 m height (Aalto et al., 2022; Scherrer & Köerner, 2010; Simin et al., 2021) greatly challenges the understanding of plant responses and feedback traditionally estimated based on T_{air}. The ignorance of accounting for the plant and air temperature differences is, however, ubiquitous, urging for correct usage of temperature to drive plant ecological processes (Körner & Hiltbrunner, 2018). Currently, no regional products exclusively describe plant temperature at different canopy heights or throughout the season. Studies using T_{surf} inevitably carry the mixed impacts of soil and snow and are restricted to only describing the canopy surface temperature for the large grids. Using a widely used ecosystem model, LPJ-GUESS, as an example, our study comprehensively assessed how using the two widely used and observation-constrained temperature products (Muñoz-Sabater et al., 2021) could lead to different estimations of water and carbon fluxes, phenological development and vegetation composition, highlighting unaccounted interactions and feedbacks from the high-latitude ecosystems when using T_{air} for all processes but also urging for community effort to put more focus on measuring plant temperature extensively and gradually developing regional products describing plant-experienced temperature.

As T_{surf} is derived from solving surface energy balance, it describes the temperature at the Earth's surface, like snow, soil or plant canopies. It also varies based on the landcover type and season. The energy balance-derived T_{surf} is close to the satellite-based land surface temperature, but it differs in that the impacts from boundary conditions and the physical environment are considered. In snow-free periods over vegetated areas, T_{surf} is close to the T_{plant} for low-statured tundra plants, but in forests with multiple canopy layers, T_{surf} only describes the uppermost layer, that is, the top canopy of the tallest trees. In the snow-covered months, neither T_{surf} nor T_{air} represents the T_{plant} during their dormancy. Under the snow cover, T_{plant} also depends on plant's stature, snow depth and topography (Körner & Hiltbrunner, 2018; von Oppen et al., 2022). Understanding the variations of T_{plant} in winter is as important as in the growing season since temperature strongly influences bud dormancy and vernalization (Larran et al., 2023).

In our analysis, the cold-biased T_{surf} in winter months mainly delayed the start of the growing season for boreal deciduous PFTs, but not for arctic PFTs with shorter growing season. To capture the dynamics of plant temperature in winter months, models need to simulate snow dynamics (Pongracz et al., 2021), leaf-level energy balance with and without snow, and thermal dynamics throughout the air-snow-plant-soil column (Martín Belda et al., 2022). Furthermore, empirical relationships and parameters calibrated based on T_{air} (such as the phenology or photosynthesis equations in LPJ-GUESS) will require further adjustments/calibration after accounting for plant temperature dynamics. LPJ-GUESS with leaf-level energy balance (Martín Belda et al., 2022) has not yet been rigorously tested for high latitudes where snow and frozen soils are present. Therefore, future investigations of the impacts of T_{plant} on ecosystem structure and carbon and water cycles are needed by integrating plant regulations and properties.

Our analysis suggests that models could underestimate high-latitude plant carbon uptake if they cannot represent the true higher-than-air plant temperatures, especially on sunny days during the active growing season. High-latitude vegetation frequently operates below its photosynthetic optimum temperatures and could greatly benefit from canopies efficiently absorbing heat to elevate its temperature, greatly promoting growth, development, and reproduction (Körner & Kèorner, 1999). Furthermore, the T_{surf}-based GPP values for boreal needle-leave PFTs could be higher than what is estimated now by LPJ-GUESS due to the annual carbon allocation scheme, in which the model cannot capture the new growth of needles during the growing season, but instead largely influenced by lower annual LAI (see Figure S3 and S4 in Supporting Information S1).

Based on the analysis of the latest CMIP6 models, high latitudes will likely experience increased temperature and precipitation, with annual shortwave radiation showing both increases and decreases (Tang et al., 2023). Under future conditions, plant traits (such as height, leaf arrangement, and canopy structural form), vegetation

composition, and canopy density will likely change, which, together with changing climate, will interactively influence the plant-to-air temperature differences. Understanding how plant temperature evolves with changing climate is a puzzle to unraveling high-latitude vegetation carbon and nutrient dynamics, and ignoring plant-to-air temperature differences might be one of the contributors to the underestimated photosynthetic carbon fixation in earth system models based on satellite data analysis (A J Winkler et al., 2019).

4. Conclusions

Our study illustrates that running ecosystem models using air or surface temperature leads to contrasting estimations of terrestrial water and carbon fluxes, phenological development and vegetation composition. Overall, surface temperature drives higher ecosystem productivity than air temperature in the Arctic tundra, mainly because of the longer growing season, higher individual productivity, and higher foliar coverage. The lower surface than the air temperature in non-summer months due to reflectivity restricts summer-season plant productivity in boreal forest regions due to lower foliar coverage and enzyme activity. This study also illustrates the contrasting impacts of temperature-induced changes in the tundra and boreal ecosystems through altering vegetation composition and individual productivity. Although surface temperature is not always a valid representation of plant temperature because canopy depth and land surface properties, such as soil and snow coverage, strongly influence it, this paper emphasizes the importance of selecting as accurate temperature data as possible to assess high-latitude ecosystem processes under the changing climate.

Conflict of Interest

The authors declare no conflicts of interest relevant to this study.

Data Availability Statement

The code version used for this study can be found in Tang et al. (2024). LPJ-GUESS input data can be found in Tang and Chen, (2024).

Acknowledgments
Y.H.F. is supported by the National Science Fund for Distinguished Young Scholars (42025101) and National key research and development program (2023YFF0805604) and the work was supported by the International Cooperation and Exchanges NSFC-STINT (42111530181), J.T. is supported by Villum Young Investigator (Grant number VIL53048), Swedish FORMAS (Forskningsråd för hållbar utveckling) mobility Grant (2016-01580), Lund University strategic research area MERGE and European Union's Horizon 2020 research and innovation programme under Marie Sklodowska-Curie (Grant 707187) and ERC consolidator grant (TUVOLU, Grant number 771012). J.T. and R.R. acknowledge the support by the Danish National Research Foundation within the Center for Volatile Interactions (VOLT, DNRF168). S.C., J.T. and Y.H.F. thank the Joint China-Sweden Mobility Program (Grant number CH2020-8656). This study was supported by the 111 Project (B18006).

References

Aalto, J., Tyystjärvi, V., Niittynen, P., Kemppinen, J., Rissanen, T., Gregow, H., & Luoto, M. (2022). Microclimate temperature variations from boreal forests to the tundra. *Agricultural and Forest Meteorology*, *323*, 109037. https://doi.org/10.1016/j.agrformet.2022.109037

ECMWF. (2016). IFS documentation – Cy41r2. In *Part IV: Physical processes*.

Good, E. J. (2016). An in situ-based analysis of the relationship between land surface "skin" and screen-level air temperatures. *Journal of Geophysical Research: Atmospheres*, *121*(15), 8801–8819. https://doi.org/10.1002/2016jd025318

Good, E. J., Ghent, D. J., Bulgin, C. E., & Remedios, J. J. (2017). A spatiotemporal analysis of the relationship between near-surface air temperature and satellite land surface temperatures using 17 years of data from the ATSR series. *Journal of Geophysical Research: Atmospheres*, *122*(17), 9185–9210. https://doi.org/10.1002/2017jd026880

Hickler, T., Smith, B., Sykes, M. T., Davis, M. B., Sugita, S., & Walker, K. (2004). Using a generalized vegetation model to simulate vegetation dynamics in northeastern USA. *Ecology*, *85*(2), 519–530. https://doi.org/10.1890/02-0344

Huang, M., Piao, S., Ciais, P., Peñuelas, J., Wang, X., Keenan, T. F., et al. (2019). Air temperature optima of vegetation productivity across global biomes. *Nature Ecology and Evolution*, *3*(5), 772–779. https://doi.org/10.1038/s41559-019-0838-x

Jones, M. B. (1985). Chapter 3 - plant microclimate. In J. Coombs, D. O. Hall, S. P. Long, & J. M. O. Scurlock (Eds.), *Techniques in bioproductivity and photosynthesis (second edition)* (pp. 26–40). Pergamon.

Körner, C. (2007). The use of 'altitude' in ecological research. *Trends in Ecology & Evolution*, *22*(11), 569–574. https://doi.org/10.1016/j.tree.2007.09.006

Körner, C. (2021). The climate plants experience, In *Alpine plant life: Functional plant ecology of high mountain ecosystems* (pp. 65–88). Springer International Publishing.

Körner, C., & Hiltbrunner, E. (2018). The 90 ways to describe plant temperature. *Perspectives in Plant Ecology, Evolution and Systematics*, *30*, 16–21. https://doi.org/10.1016/j.ppees.2017.04.004

Körner, C., & Kèorner, C. (1999). Alpine plant life: Functional plant ecology of high mountain ecosystems.

Larran, A. S., Pajoro, A., & Qüesta, J. I. (2023). Is winter coming? Impact of the changing climate on plant responses to cold temperature. *Plant, Cell and Environment*, *46*(11), 3175–3193. https://doi.org/10.1111/pce.14669

La Sorte, F. A., Johnston, A., & Ault, T. R. (2021). Global trends in the frequency and duration of temperature extremes. *Climatic Change*, *166*(1), 1. https://doi.org/10.1007/s10584-021-03094-0

Martín Belda, D., Anthoni, P., Wårlind, D., Olin, S., Schurgers, G., Tang, J., et al. (2022). LPJ-GUESS/LSMv1. 0: A next-generation land surface model with high ecological realism. *Geoscientific Model Development*, *15*(17), 6709–6745. https://doi.org/10.5194/gmd-15-6709-2022

Muñoz Sabater, J. (2019). ERA5-Land hourly data from 1950 to present. [Dataset]. https://doi.org/10.24381/cds.e2161bac

Muñoz-Sabater, J., Dutra, E., Agustí-Panareda, A., Albergel, C., Arduini, G., Balsamo, G., et al. (2021). ERA5-Land: A state-of-the-art global reanalysis dataset for land applications. *Earth System Science Data*, *13*(9), 4349–4383. https://doi.org/10.5194/essd-13-4349-2021

Piao, S., Liu, Q., Chen, A., Janssens, I. A., Fu, Y., Dai, J., et al. (2019). Plant phenology and global climate change: Current progresses and challenges. *Global Change Biology*, *25*(6), 1922–1940. https://doi.org/10.1111/gcb.14619

Pongracz, A., Wårlind, D., Miller, P. A., & Parmentier, F.-J. W. (2021). Model simulations of arctic biogeochemistry and permafrost extent are highly sensitive to the implemented snow scheme in LPJ-GUESS. *Biogeosciences*, *18*(20), 5767–5787. https://doi.org/10.5194/bg-18-5767-2021

Pugh, T. A., Arneth, A., Kautz, M., Poulter, B., & Smith, B. (2019). Important role of forest disturbances in the global biomass turnover and carbon sinks. *Nature Geoscience*, *12*(9), 730–735. https://doi.org/10.1038/s41561-019-0427-2

Rinnan, R., Iversen, L. L., Tang, J., Vedel-Petersen, I., Schollert, M., & Schurgers, G. (2020). Separating direct and indirect effects of rising temperatures on biogenic volatile emissions in the Arctic. *Proceedings of the National Academy of Sciences*, *117*(51), 32476–32483. https://doi.org/10.1073/pnas.2008901117

Scherrer, D., & Körner, C. (2010). Infra-red thermometry of alpine landscapes challenges climatic warming projections. *Global Change Biology*, *16*(9), 2602–2613. https://doi.org/10.1111/j.1365-2486.2009.02122.x

Seyednasrollah, B., Young, A. M., Li, X., Milliman, T., Ault, T., Frolking, S., et al. (2020). Sensitivity of deciduous forest phenology to environmental drivers: Implications for climate change impacts across north America. *Geophysical Research Letters*, *47*(5), e2019GL086788. https://doi.org/10.1029/2019gl086788

Simin, T., Tang, J., Holst, T., & Rinnan, R. (2021). Volatile organic compound emission in tundra shrubs–Dependence on species characteristics and the near-surface environment. *Environmental and Experimental Botany*, *184*, 104387. https://doi.org/10.1016/j.envexpbot.2021.104387

Sitch, S., Smith, B., Prentice, I. C., Arneth, A., Bondeau, A., Cramer, W., et al. (2003). Evaluation of ecosystem dynamics, plant geography and terrestrial carbon cycling in the LPJ dynamic global vegetation model. *Global Change Biology*, *9*(2), 161–185. https://doi.org/10.1046/j.1365-2486.2003.00569.x

Smith, B., Wårlind, D., Arneth, A., Hickler, T., Leadley, P., Siltberg, J., & Zaehle, S. (2014). Implications of incorporating N cycling and N limitations on primary production in an individual-based dynamic vegetation model. *Biogeosciences*, *11*(7), 2027–2054. https://doi.org/10.5194/bg-11-2027-2014

Still, C., Powell, R., Aubrecht, D., Kim, Y., Helliker, B., Roberts, D., et al. (2019). Thermal imaging in plant and ecosystem ecology: Applications and challenges. *Ecosphere*, *10*(6), e02768. https://doi.org/10.1002/ecs2.2768

Sykes, M. T., Prentice, I. C., & Cramer, W. (1996). A bioclimatic model for the potential distributions of north European tree species under present and future climates. *Journal of Biogeography*, *23*(2), 203–233. https://doi.org/10.1046/j.1365-2699.1996.d01-221.x

Tang, J., & Chen, S. (2024). Model data linked to the paper "Air and surface temperatures differently drive terrestrial carbon and water cycles in the high latitudes". [Dataset]. University of Copenhagen. https://doi.org/10.17894/UCPH.9537069C-A4C5-4B2F-851D-785621FCD760

Tang, J., Chen, S., & Fu, Y. (2024). Air and surface temperatures differently drive terrestrial carbon and water cycles in the high latitudes [Software]. *Zenodo*. https://doi.org/10.5281/zenodo.10726860

Tang, J., Zhou, P., Miller, P. A., Schurgers, G., Gustafson, A., Makkonen, R., et al. (2023). High-latitude vegetation changes will determine future plant volatile impacts on atmospheric organic aerosols. *NPJ Climate and Atmospheric Science*, *6*(1), 147. https://doi.org/10.1038/s41612-023-00463-7

Vitasse, Y., Baumgarten, F., Zohner, C. M., Kaewthongrach, R., Fu, Y. H., Walde, M. G., & Moser, B. (2021). Impact of microclimatic conditions and resource availability on spring and autumn phenology of temperate tree seedlings. *New Phytologist*, *232*(2), 537–550. https://doi.org/10.1111/nph.17606

von Oppen, J., Assmann, J. J., Bjorkman, A. D., Treier, U. A., Elberling, B., Nabe-Nielsen, J., & Normand, S. (2022). Cross-scale regulation of seasonal microclimate by vegetation and snow in the Arctic tundra. *Global Change Biology*, *28*(24), 7296–7312. https://doi.org/10.1111/gcb.16426

Winkler, A. J., Myneni, R. B., Alexandrov, G. A., & Brovkin, V. (2019). Earth system models underestimate carbon fixation by plants in the high latitudes. *Nature Communications*, *10*(1), 885. https://doi.org/10.1038/s41467-019-08633-z

Winkler, D. E., Butz, R. J., Germino, M. J., Reinhardt, K., & Kueppers, L. M. (2018). Snowmelt timing regulates community composition, phenology, and physiological performance of alpine plants. *Frontiers in Plant Science*, *9*, 1140. https://doi.org/10.3389/fpls.2018.01140

Zohner, C. M., Mirzagholi, L., Renner, S. S., Mo, L., Rebindaine, D., Bucher, R., et al. (2023). Effect of climate warming on the timing of autumn leaf senescence reverses after the summer solstice. *Science*, *381*(6653), eadf5098. https://doi.org/10.1126/science.adf5098